

STATIC, DYNAMIC AND SEISMIC PERFORMANCE OF NOVEL CROSS – SECTION DINOBEAM

Farsana Samad¹, Geethika G Pillai²

¹P.G Student, Dept of Civil Engineering, Indira Gandhi Institute of Polytechnic and Engineering, Nellikkuzhy, Ernakulam, Kerala, India

²Assistant Professor, Dept. Of Civil Engineering, Indira Gandhi Institute of Polytechnic and Engineering, Nellikkuzhy, Ernakulam, Kerala, India

Abstract – This project aims to study the development of a steel beam with a novel dog-bone shaped cross-section, referred to as the Dinobeam. The Dinobeam is intended for use as a secondary floor beam in high-rise construction, capable of spanning distances greater than 12 m. The primary advantage of the Dinobeam cross-section is the fact that its closed hollow flanges give the cross-section increased resistance to lateral torsion buckling compared to the typical I-cross section. In this study flexural testing, low velocity impacts as dynamic and seismic performance in multistory frame are conducted to evaluate the performance against the sustainability and also with comparison of conventional section. The output parameters like ultimate load, deflection, stiffness, ductility, lateral resisting strength index, collapse failure are evaluated using nonlinear finite element method using ANSYS software.

Key Words: Dinobeam and Conventional beam- Static Analysis- Dynamic analysis- Vibrational Analysis- Seismic Analysis- ANSYS

1. INTRODUCTION

Research is a process of arriving at an appropriate solution to a problem through development of a new type of steel beam structure with novel dog-bone shaped cross-section, to be referred to as the Dinobeam. The cross-section is envisioned to be a light-weight alternative to the typical I cross-section intended for use in secondary floor beams where the required span between supports is greater than 12 m. The nomenclature used for the Dinobeam geometry. The Dinobeam cross-section has several advantages compared an I cross-section. Firstly, the hollow flanges provide the Dinobeam with an increased resistance to lateral-torsion buckling failure, the primary failure mechanism in long spanning beams. Consequently a smaller, and therefore lighter Dinobeam cross-section could be used in the place of an I cross-section. Another advantage is the fact that, apart from the top of the top flange, the Dinobeam has no upwards facing horizontal surfaces. This means that for when the beam is used to support a floor slab or roof system sitting directly on top of the top flange, there is no surface for birds or other animals to sit. .

It is intended that designers will be able to optimize the Dinobeam cross-section for any given span and loading conditions by changing the depth of the flange and width of the flange. In this study flexural testing, model analyses as dynamic and seismic performance in multistory frame are conducted to evaluate the performance against the sustainability and also with comparison of conventional section. The output parameters like ultimate load, deflection, stiffness, ductility, lateral resisting strength index, collapse failure are evaluated using nonlinear finite element method using ANSYS software.

2. FLEXURAL TESTING AND PARAMETRIC STUDY

2.1 GENERAL

Dinobeam and Conventional beam models are taken for performing the flexural testing and the values are compared between them. For parametric study of Dinobeam by varying depth of flange, width of flange and height of flange and compared between the actual Dinobeam model.

2.2 GEOMETRY AND BOUNDARY CONDITIONS

Dinobeam of dimension ETF-450x150-tf6-tw8-N200-A0 and Conventional beam of dimension ISWB 400 models are used. To stimulate the real conditions, Dinobeam model and Conventional beam models are analysed with simply supported system at both ends and load is applied as two-point loading in one direction at L/3 distance from both ends.

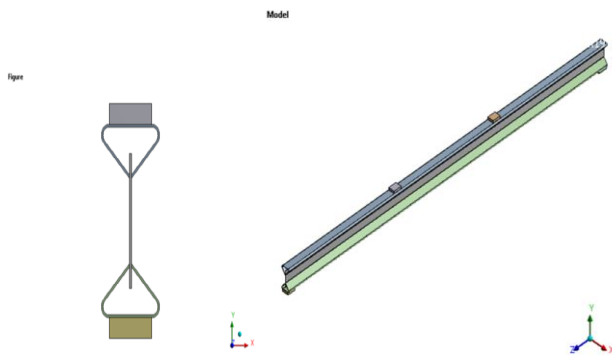


Fig-1: Geometry of Dinobeam

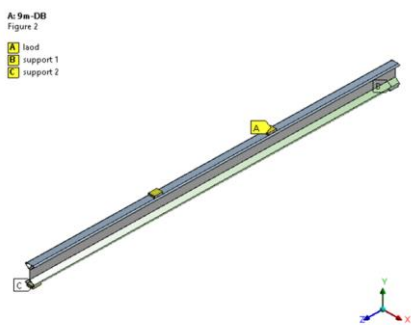


Fig-2: Boundary condition of Dinobeam

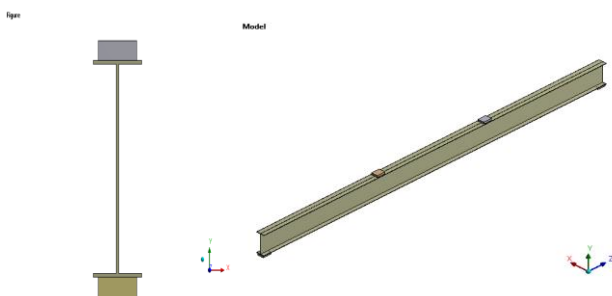


Fig-3: Geometry of Conventional beam

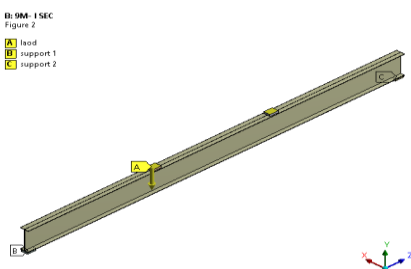


Fig-4: Boundary condition of Conventional beam

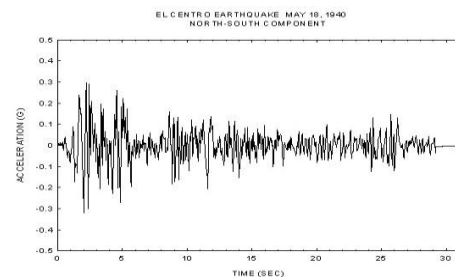
2.3 MATERIAL PROPERTIES

Dinobeam and Conventional beam have same material properties. Young's modulus is $2e5$ MPa, density is 7750 Kg/m³ and Poisson's ratio is 0.3.

3. VIBRATIONAL ANALYSIS AND SEISMIC ANALYSIS

3.1 GENERAL

Dinobeam structure and Conventional beam structure of 5 bays and 10 storeys are modelled to perform the vibrational analysis and seismic analysis. Elcentro earthquake (Time History Data File Reference: Pacific Earthquake Engineering Research Center <http://peer.berkeley.edu/research/motions>) passing through this two structures and finding the model analysis(time period and frequency) and time history analysis(storey displacement, base shear and acceleration).



Time History Data File Reference:
Pacific Earthquake Engineering Research Center
<http://peer.berkeley.edu/research/motions>

Fig-5: Elcentro earthquake graph

3.1 GEOMETRY AND BOUNDARY CONDITIONS

Dinobeam structure and Conventional beam structure of 5 bays and 10 storeys are modelled to perform the vibrational analysis and seismic analysis. The columns used in these buildings are Indian Standard Wide Flange Beam 400 (ISWB 400).

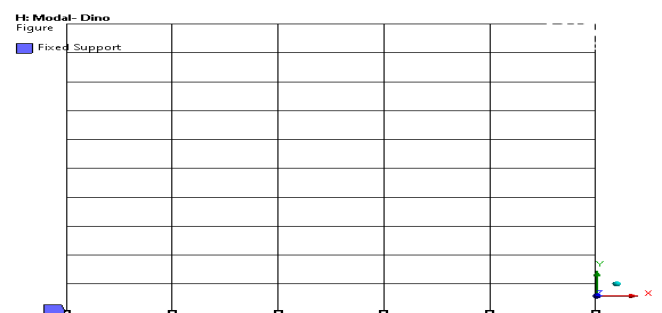


Fig-6: Geometry of multi-storey frame

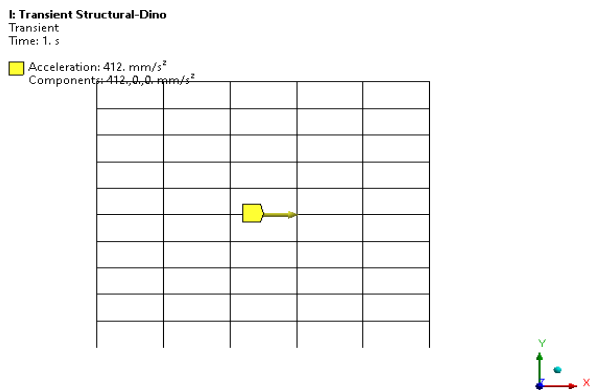


Fig-7: Boundary conditions of multi-storey frame

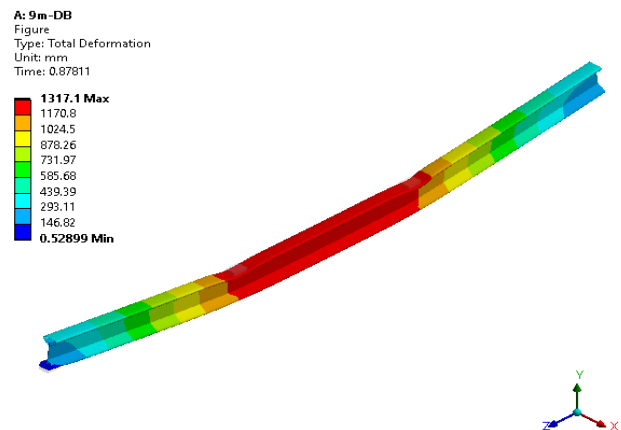


Fig-8: Total deformation of Dinobeam model in flexural testing

4. RESULT AND DISCUSSION

4.1 FLEXURAL TESTING AND PARAMETRIC STUDY

Dinobeam model and Conventional beam model were subjected to two-point loading which undergoes flexural testing and parametric study of beams by varying depth of flange and width of flange by increasing and decreasing 25mm and by varying full height of web. The weights of the models are same. The models were simply supported at a distance of 9000mm from both the ends and loads were applied at a distance of 3000mm from both ends of the model

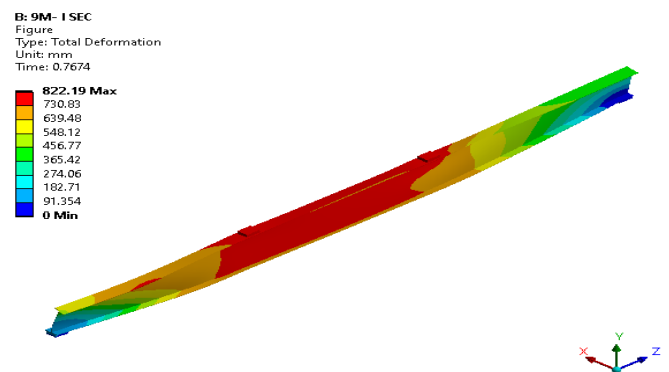


Fig-9: Total deformation of Conventional beam model in flexural testing

Table -1: Ultimate load and total deformation of beam models under flexural testing

Model	Dinobeam	Conventional beam
Ultimate Yielding (mm)	112.98	18.55
Ultimate deflection (mm)	1317.10	822.19
Ultimate load (KN)	365.18	360.27
Percentage of increase in load (%)	1.00	1.36
Ductility	TORISON BUCKLING	11.66

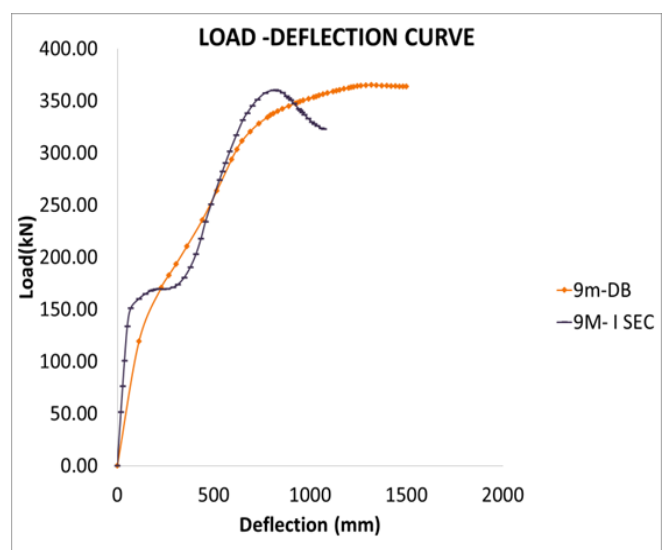


Fig-10: Load deflection graph of beams which undergo flexural testing

Table -2: Ultimate load and total deformation of beam models in parametric study

SL. NO:	Model	Parametric study of beam	Ultimate yielding (mm)	Ultimate deflection (mm)	Ultimate load (KN)	Percentage of increase in load(%)	Ductility	
1	Dinobeam	Actual model	112.98	1317.1	365.18	1	TORISON BUCKLIN	
		By varying depth of flange	DB-FD= +25MM	110.26	917.43	413.14	14.68	8.32
			DB-FD= -25MM	112.12	1372.2	377.53	4.79	12.24
		By varying width of flange	DB-FW +25MM	111.56	1413.8	390.09	8.28	12.67
			DB-FW -25MM	110.35	868.21	385.28	6.94	7.87
By varying height of web	DB-FULL WEB	112.76	826.17	387.57	7.58	7.33		
2	Conventional beam	I section	18.55	822.19	360.27	1.36	11.66	

G: 9m-DB-FD= +25MM
Figure
Type: Total Deformation
Unit: mm
Time: 0.60532

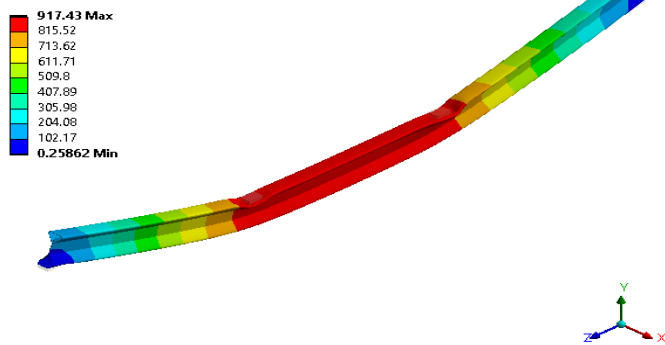


Fig-11: Total deformation of Dinobeam model in parametric study (DB-FD=+25mm)

F: 9m-DB-FD= -25MM
Figure
Type: Total Deformation
Unit: mm
Time: 0.91475

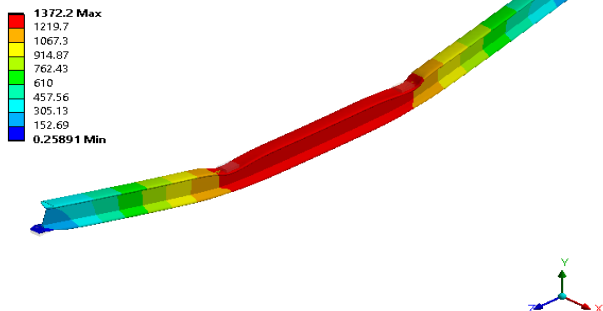


Fig-12: Total deformation of Dinobeam model in parametric study (DB-FD=-25mm)

G: 9m-DB-FD= +25MM
Figure
Type: Total Deformation
Unit: mm
Time: 0.60532

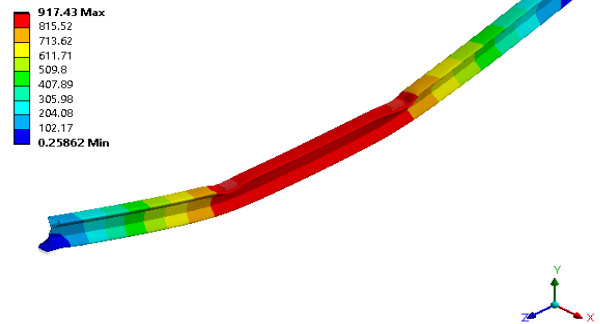


Fig-13: Total deformation of Dinobeam model in parametric study (DB-FW=+25mm)

D: 9m-DB-FW= -25MM
Figure
Type: Total Deformation
Unit: mm
Time: 0.96319

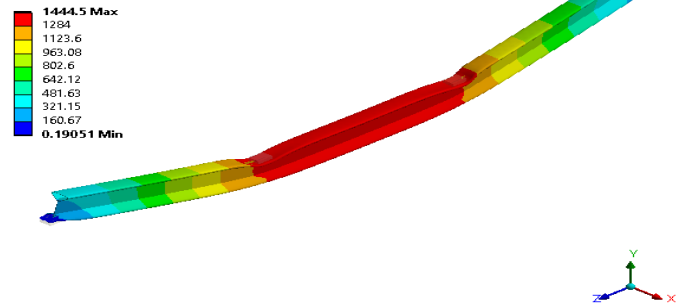


Fig-14: Total deformation of Dinobeam model in parametric study (DB-FW=-25mm)

C: 9m-DB-FULL WEB
Figure
Type: Total Deformation
Unit: mm
Time: 0.55041

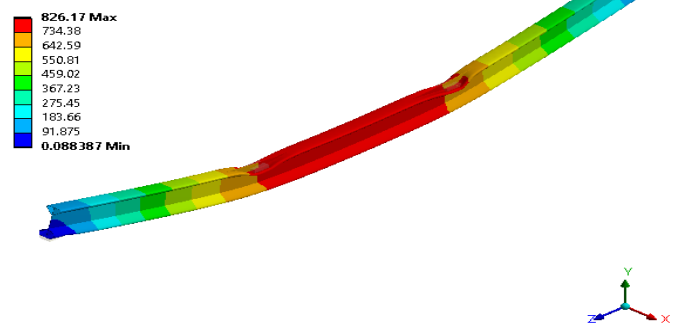


Fig-15: Total deformation of Dinobeam model in parametric study (DB-FULL WEB=+25mm)

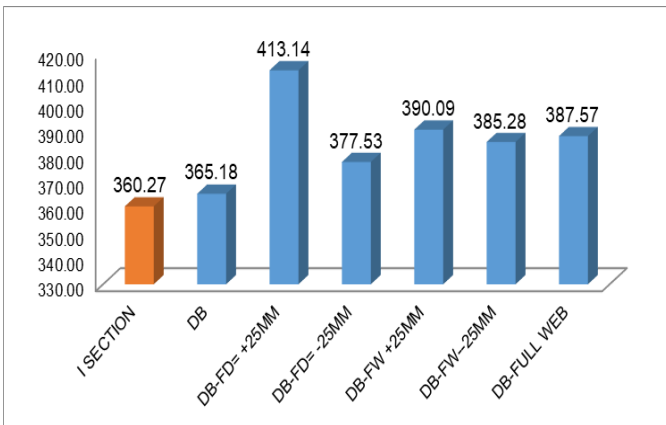


Fig-16: Load comparison chart

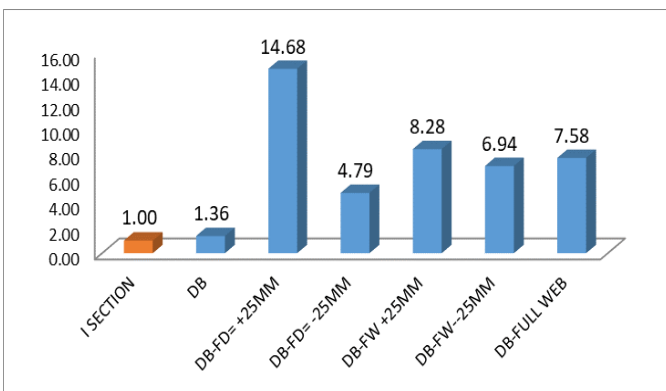


Fig-17: Percentage of increase in load

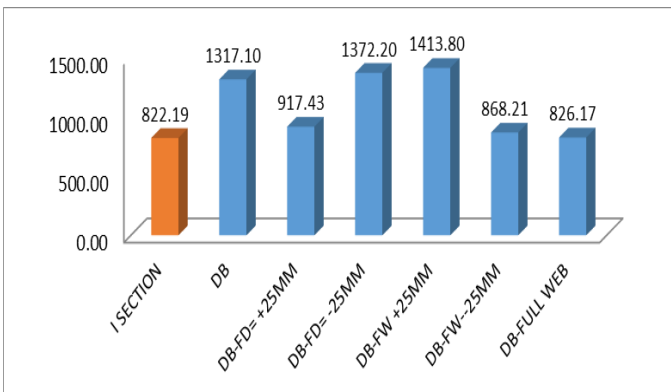


Fig-18: Deformation chart

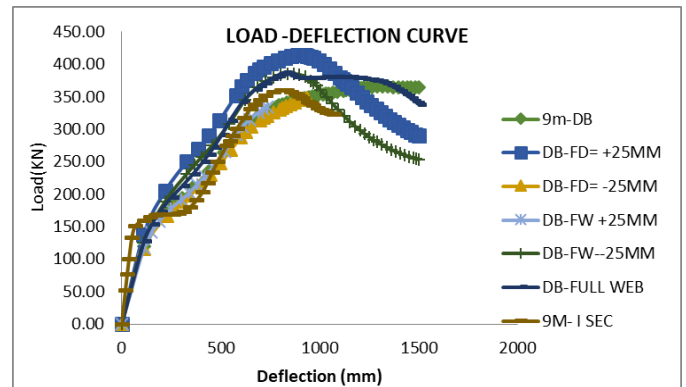


Fig-19: Load deflection graph of beam which undergo parametric study

4.2 VIBRATIONAL ANALYSIS AND SEISMIC ANALYSIS

Dinobeam model and Conventional beam model were used to build 2 separate multi-storey frames of 5 bays and 10 storeys. The weights of the models are same and the Elcentro earthquake is passing through the frames and also which beam model frame faces the failure easily can be identified and compared between them.

Table -3: Model Analysis of beam models

Model	Dinobeam	Conventional beam
Frequency (Hz)	1.566	1.4
Time Period (s)	0.638569604	0.714285714

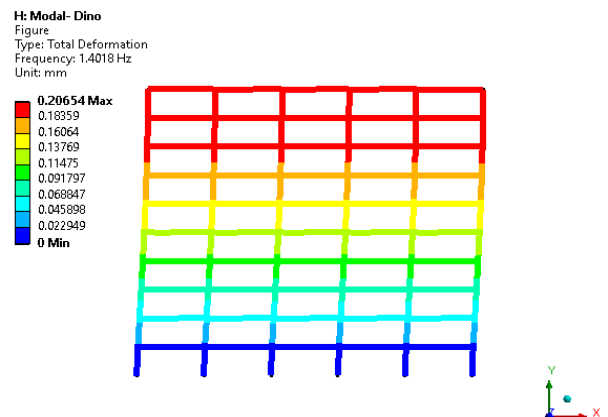


Fig-20: Total deformation of Dinobeam-multi-storey frame in model analysis

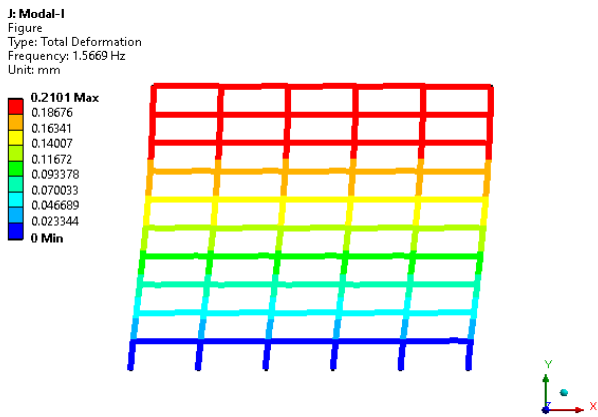


Fig-21: Total deformation of Conventional-multi-storey frame in model analysis

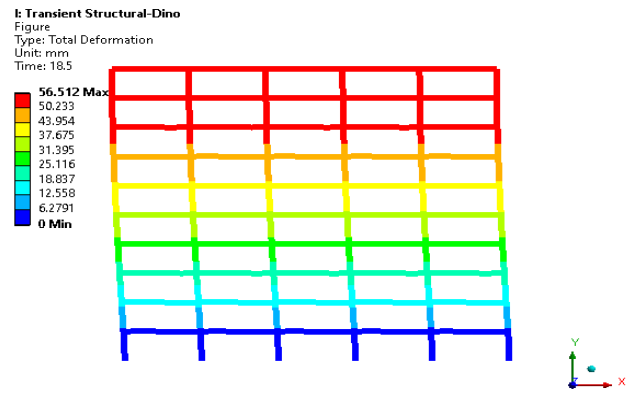


Fig-23: Total deformation of Dinobeam-multi-storey frame in time history analysis

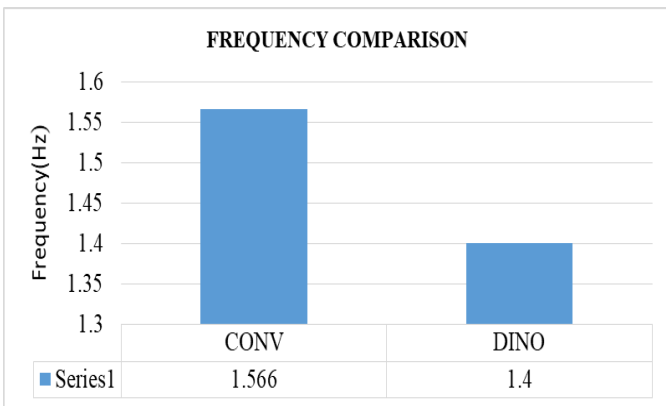


Fig-22: Frequency comparison chart

Table -4: Time History Analysis of beam models

Model	Dinobeam	Conventional beam
Storey Displacement (mm)	49.7	56.52
Base Shear (N)	15519	13179
Acceleration (mm/s ²)	1703	1368.6

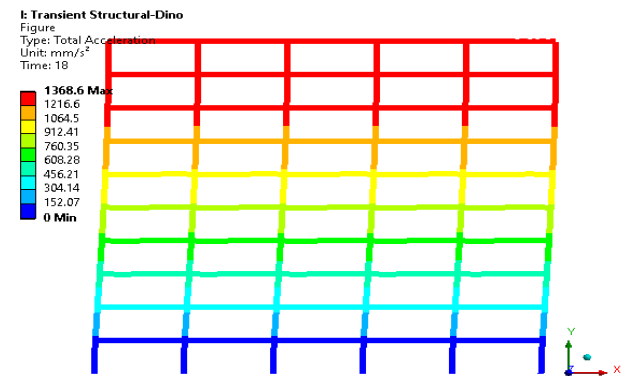


Fig-24: Total acceleration of Dinobeam-multi-storey frame in time history analysis

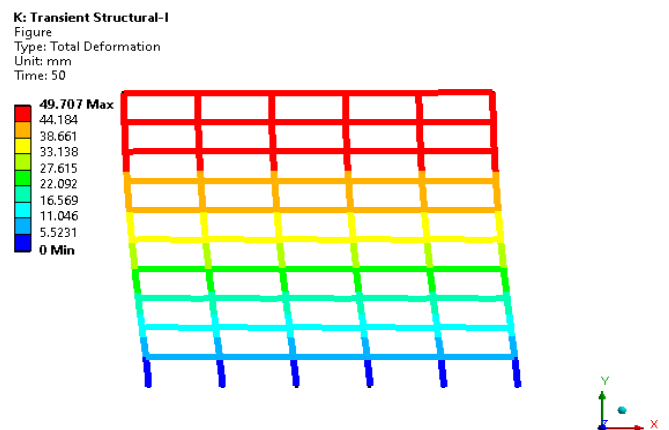


Fig-25: Total deformation of Conventional-multi-storey frame in time history analysis

K: Transient Structural-1
Total Acceleration
Type: Total Acceleration
Unit: mm/s²
Time: 53.5

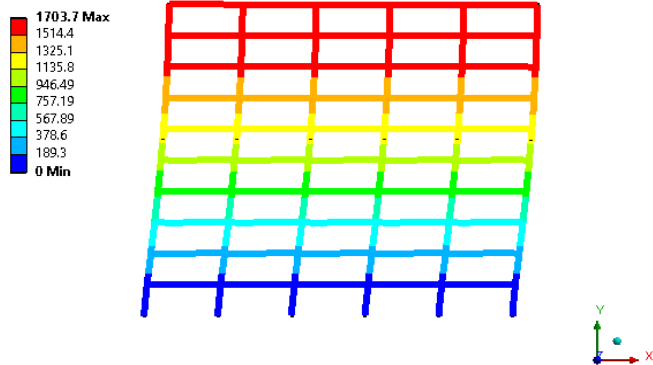


Fig-26: Total acceleration of Conventional-multi-storey frame in time history analysis

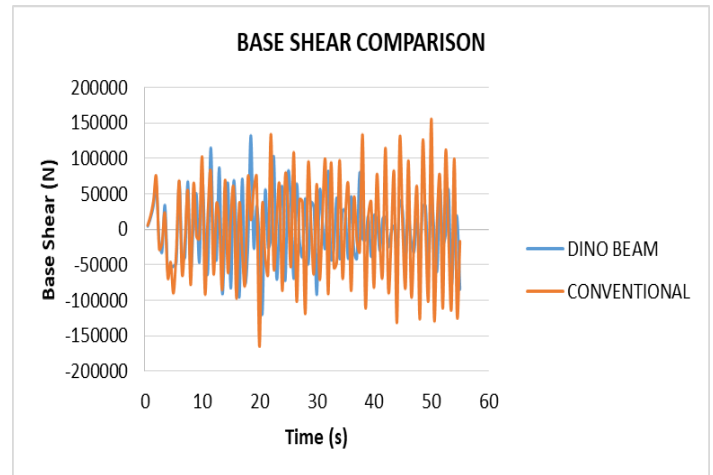


Fig-29: Base shear comparison graph

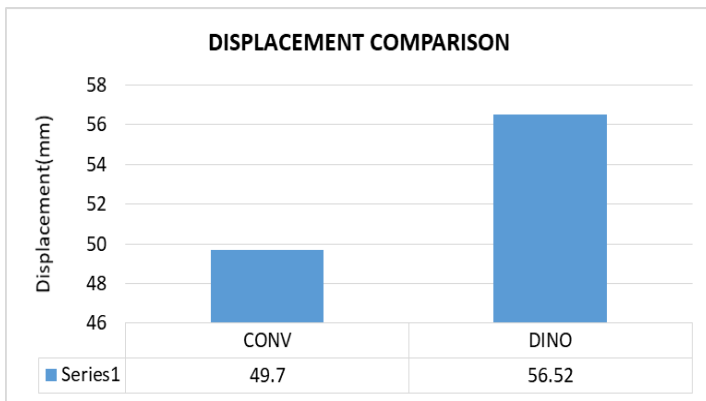


Fig-27: Displacement comparison chart

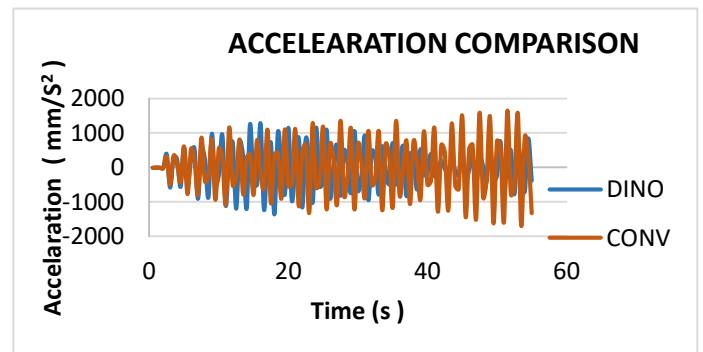


Fig-30: Acceleration comparison graph

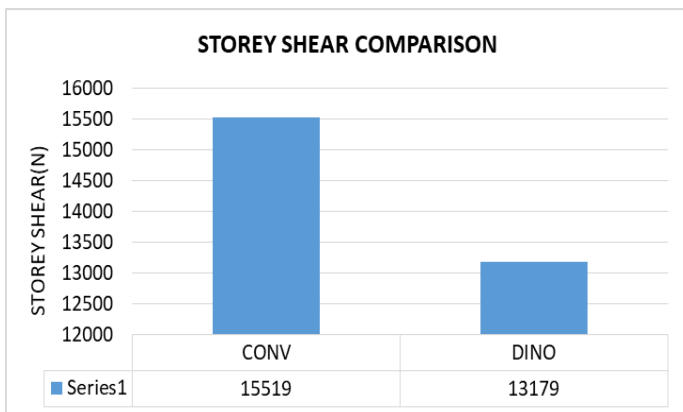


Fig-28: Storey shear comparison chart

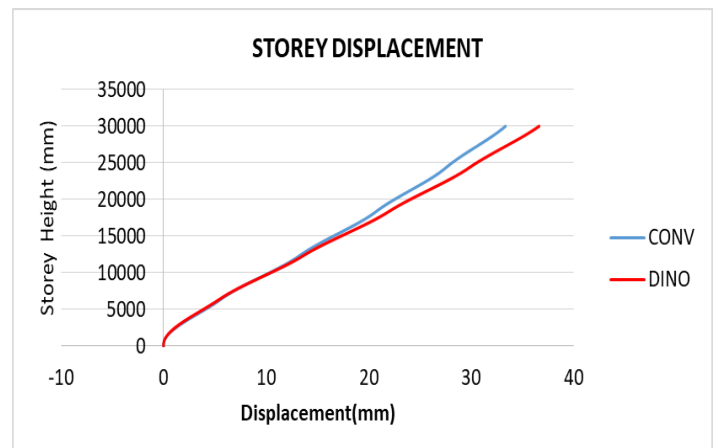


Fig-31: Storey displacement graph

5. CONCLUSIONS

The following conclusions are made from the study:

- 1 In flexural testing, Conventional beam model deformed quickly so the failure occurs faster than Dinobeam model here torsion buckling happens in I section.

2. In parametric study of Dinobeam by varying depth of flange by increasing 25mm, Dinobeam model shows 14.68% increase in load carrying capacity while varying width of flange by decreasing 25mm, Dinobeam model shows increase in ductility compared to actual Dinobeam model.

3. While comparing the parameters, web performance is very less. Flange is the important parameter than web because of flange dimensions are not important here than web dimensions.

4. In performing the vibrational characteristics of multi-storey frame, Dinobeam frame shows 11% more time period than Conventional beam frame. While frequency is less in Dinobeam frame than Conventional beam frame. This shows the Dinobeam structure is flexible.

5. In seismic/ earthquake analysis, Dinobeam frame has less acceleration and base shear that means the stiffness is less and the damping is more so the building can withstand more seismic force and energy dissipation will be high.

REFERENCES

- [1] Matthew J. Russell, James B.P. Lim, Krishanu Roy, G. Charles Clifton, Jason M. Ingham .Welded steel beam with novel cross-section and web openings subject to concentrated flange loading. Department of Civil and Environmental Engineering, University of Auckland, Auckland, New Zealand. *Struct*2020;24:580-599
- [2] Roy K, Mohammad, jani C, Lim JBP. Experimental and numerical investigation into the behaviour of face-to-face built-up cold-formed steel channel sections under compression. *Thin-Walled Struct*2019; 134:291–309.
- [3] Krishnanu Roy, JBP, Lim. Numerical investigation into the buckling behaviour of face-to-face built-up cold-formed stainless steel channel sections under axial compression. *Struct*2019; vol.20.p.42-73.
- [4] Roy K, Ting TCH, Lau HH, Lim JBP. Nonlinear behaviour of back-to-back gapped built-up cold-formed steel channel sections under compression. *J Constr Steel Res* 2018; 147:257–76.
- [5] Giuseppe Roy K, Ting TCH, Lau HH, Lim JBP. Nonlinear behavior of axially loaded back-toback built-up cold-formed steel un-lipped channel sections. *Steel Compos StructInt J* 2018; 28(2):233–50.